2020 11th International Conference on Electrical and Computer Engineering (ICECE)

Minimally produced inkjet-printed tactile sensor model for improved data reliability

Steven D. Gardner*, J. Iwan D. Alexander*, Yehia Massoud†, and Mohammad R. Haider*
*School of Engineering, University of Alabama at Birmingham, Birmingham, AL, USA
†School of Systems and Enterprises, Stevens Institute of Technology, Hoboken, NJ, USA
{stevendg, ialex, mrhaider}@uab.edu, ymassoud@stevens.edu

2020 11th International Conference on Electrical and Computer Engineering (ICECE) | 978-1-6654-2254-3/20/$31.00 ©2020 IEEE | DOI: 10.1109/ICECE51571.2020.9393138

***Abstract*—Inkjet-printing as an on-the-go, inexpensive, and green method of creating instant flexible sensors and circuits will not proliferate until reliable device fabrication is possible outside the research environment. Shortfalls exist due to non-uniform fabrication/curing, environmental humidity/temperature influence, and uncontrollable deposition conditions, particularly in low-production setups. Electrical non-uniformity and variations from low-quality prints made by a minimally produced inkjet-printed sensor may be overcome by training a machine learning model to interpret the variabilities and output a high-confidence prediction of the signal. In this report, an inkjet-printed tactile sensor is modeled to simulate generate a rich data-set for training and testing an echo state network. The end goal of the reported work is to attach the echo state network to the imperfect, on-the-go, inkjet-printed sensor as an edge computing device, transforming the unreliable data into a more stable readout. In this way, the sensor design may be printed using any suitable inkjet-printer with minimal production effort and still extract reliable data. This enables inkjet-printers to be used at home by those in isolated/restrictive settings, poor communities, resource starved environments, or by enthusiasts. Applications include biometric, environmental, electro-chemical and -mechanical sensing, and the concept may be extended to inkjet-printed circuits for signal stabilization.**

***Index Terms*—inkjet printed tactile sensor, biosensor, reservoir computing, MATLAB simulation**

I. Introduction

The widespread availability and usage of 3D-printing opened opportunities for fabrication settings away from the research domain, in homes, workshops, and remote/isolated places like upon the ISS [1]. Additionally, increased demand has brought about competition, lowered prices and improved support both technically and within newly formed communities of enthusiasts. Inkjet-printing (IJP) using nanoparticle inks has the potential to proliferate in the same manner as 3D printing. While IJP is a well-established ink deposition method, the introduction of metal, semiconducting, insulator, and other exotic nanoparticle inks has revitalized their usefulness.

Recent market trends show increased demand of printed electronics for smart and connected devices, and a rise in the demand for energy-efficient, thin, cost-effective and flexible consumer electronics [2]. Inkjet-printing is the most popular method of additive manufacturing, requiring no etching, hazardous wastes, and often results in biodegradable devices, making it environmentally friendly [3], [4]. Flexible sensors, circuits and electrical routing can instantly be printed by IJP, and when combined with a 3D-printer, custom-made and fully packaged electronics can be fabricated within hours [5].

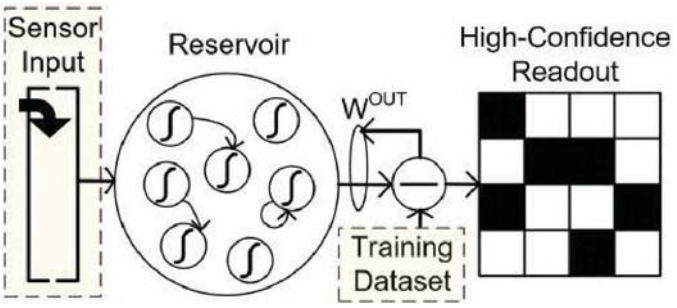

Fig. 1: The ESN architecture is shown. A signal is input to the trained neural network and the predicted output dataset is visualized (far right). The shaded areas establish the scope of this report.

Unfortunately, inkjet-printing has several shortfalls that restrict its ability to grow in the same manner as 3D printing, including lagging industry response to demand, substantial amount of resources needed to fabricate reliable prints, limited commercially-available inks and lacking printer support. Previous research on this topic has indicated that variabilities from fabrication, curing, and the environment cause electrical parameters hard to control. Mitigating those variabilities is important to improve sensor function and data quality for the minimal IJP process as described in Section II.

An approach to overcoming the existing pitfalls is with the support of machine learning (ML) methods to pseudo-calibrate the sensors such that their low-quality data is transformed to a high-confidence classification or time-series prediction. The proposed ML method to handle IJP sensors in this report is called reservoir computing (RC), created by H. Jaeger [6] and W. Maass [7] in 2001 and 2002, respectively. The RC architecture (shown in Fig. 1) is robust against noise and highly adaptable to work with non-conventional sensors like the IJP sensor described in this report (refer to Section II). The benefits of having the IJP sensor connected to the edge computing machine include real-time low-level processing for time-series prediction, reduced sensor noise and variability, extended sensor lifetime, minimized power and memory requirements, and the high-volume data throughput of

978-1-6654-2254-3/20/$31.00 ©2020 IEEE

the collective wireless sensor network (WSN) is reduced. Only a few papers have considered post-processing of IJP sensors as a means of data quality improvement [5], [8]–[10], and fewer consider the RC network (RCN) as an edge computing framework for *in situ* sensor data quality enhancement and volume reduction. With these motivations, a path is proposed that seeks to promote the proliferation of "on-the-go" IJP microfabrication setups.

The scope of this paper is creating the dataset for training and testing the RCN, which involves simulation and analysis of the sensor's metrics. Future works will entail training and testing the RCN, but does not lie within this report. The RCN in Fig. 1 depicts a standard echo state network (ESN). The reservoir is a recurrent neural network of leaky integrator neurons, which acts to transform the linear data into a high-dimensional state space where read-out neurons are trained to understand the reservoir states. The output of the RCN is a classification of the pattern touched on the IJP tactile sensor. In this paper, a minimally produced inkjet-printed tactile sensor is introduced in Section II, explored for metrics in Section III, and is then modeled in MATLAB and analyzed in Section IV. Lastly, Section V summarizes the report and establishes plans for future work.

II. Minimal Process IJP Sensor

Inkjet-printed pressure [11], touch [12], and proximity [13] sensors exist that are formed from only silver nanoparticle ink. Our research group has studied an IJP pressure sensor that uses a semiconductive nanoparticle sensitive to piezoelectric variations [14], [15]. Adaptations from that design allowed for a tactile (touch) sensor that only uses the silver nanoparticle ink, the fabrication of which will be shown here after establishing the basics to the process.

A. Basic IJP Fabrication Requirements and Process

The most minimal IJP microfabrication setup requires an office-quality inkjet printer with proper nozzle head size for the nanoparticle inks (est. $300), refillable ink cartridges (est. $10 per set), nanoparticle inks (est. $130 to $380 per bottle), flexible polymer substrate such as thermally resistant photopaper or polyethylene terephthalate (PET) film (est. $20 per pack), a curing method such as an oven or hot-plate (est. $20), and any editing program like CAD software, Visio, Microsoft Publisher/Paint, or other free programs. All of these form a starting budget of less than $500 when considering a setup with only silver nanoparticle ink. The entire micro-fabrication setup takes up an area of approximately 3 square feet, making it compatible for usage in compact areas.

The basic IJP process follows four steps: (1) the patterns are designed on an editing program, (2) nanoparticle inks are filled into the refillable cartridges, (3) the pattern is printed layer-by-layer, and (4) the print is thermally cured for sintering and continuous bulk formation. This process varies in research settings to include involved and expensive processes/equipment such as plasma and gas treatment,

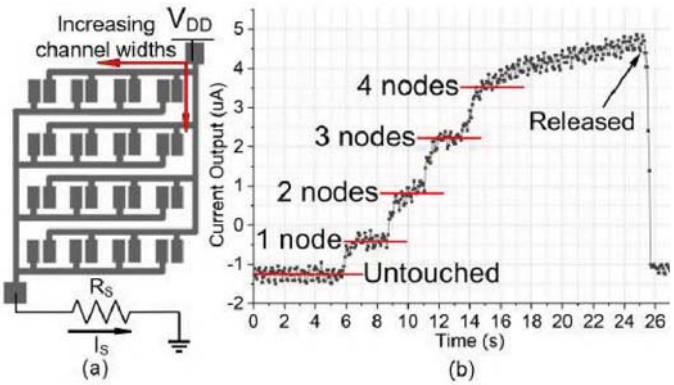

Fig. 2: (a) The IJP tactile sensor pattern is shown with its electrical equivalent overlayed. The nodes have different channel widths as a method of distinguishing them. (b) The plot shows the sensor's response when four of the 16 nodes are pressed, demonstrating that current I_S through R_S is the sum of the nodes.

non-IJP deposition (e.g. gravure, screen, flexographic printing, etc.), spin-coating, magnetron sputtering, slot-die coding, precise parameter control (e.g. ink layer thickness, cartridge temperature, nozzle head size, etc.), usage of novel materials, and many other custom processes and techniques [16]. In the large majority of reports, the inkjet printer used is the Dimatix Materials Printer (DMP), which is extremely expensive and not reasonable for minimal setups. Thus, the minimal setup was used to fabricate the tactile sensor.

B. IJP Tactile Sensor Fabrication

The IJP sensor of Fig. 2 was printed, cured and tested in the BioInspired Integrated Circuits (BIC) laboratory at the University of Alabama, Birmingham. The silver nanoparticle ink is from Mitzubishi Paper Mills Inc. (model NBSIJ-MU01). The ink was printed onto glossy photo-paper substrate using a Brother MFC-J5910DW inkjet printer. After printing, the sensor cured on a hotplate at 160 ^{o}C for 15 minutes [17]. The cost per sensor is approximately $0.09, and is a representation of the sensors expected from microfabrication setups in limited environments. Tests were performed using a Keithley 2604B Dual SourceMeter, MATLAB and the NI ELVIS II+ prototyping board. The power supply, V_{DD}, was 5V for all tests, making power output on the order of micro-Watts (10^{-6}). Power could also be reduced to 3.3V for usage with microprocessors.

III. Sensor Behavior and Metrics for Modeling

The sensor of Fig. 2 is an adaptation to a previously studied pattern [14], [15]. There, it was found that the non-uniform fabrication and uneven curing caused each node to have slightly different channel resistances. Since the nodes have a distinctive property, the ESN will have a better chance of identifying the pressed node pattern. To enhance and control this effect, the design in Fig. 2 was made to have increasing channel widths among the nodes, forming a gradient of channel resistances as depicted in Fig. 3. The values are then

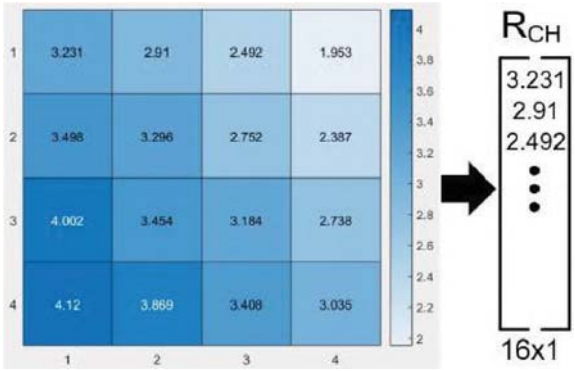

Fig. 3: Channel resistances between nodes is made to be a gradient by having the channel width increase from node to node, distinguishing them for classification. The values are stored in an array that becomes an input feature to the ESN. Resistances are in mega-Ohms ($M\Omega$).

stored in an array and will later be used as a input feature for the ESN. In the MATLAB program where this sensor is being simulated, an array of channel resistances is generated for each simulated sample by applying uniformly distributed Gaussian noise to empirically gathered channel resistances.

I_S is the main input feature to the ESN, with the channel resistance vector being a second feature to help the ESN classify the signal. Generating I_S means modeling a single node's response, applying bounded random conditions for signal variation, generating a pattern mask, populating a matrix with the randomized node response and pattern mask, and finally summing the contents of the node matrix to create the final input signal.

A. Single Node Profile

Empirical tests show the profile of a node when it is touched (black line of Fig. 4). The signal starts with a bias current and when touched, current flow steeply rises, saturates and flattens for the duration of being touched before dropping back down to the bias current when the node is released. There is a linear rise after the signal has saturated since thermal energy from the finger is absorbed into the substrate, causing channel resistance to gradually decrease and current to increase. These basic behaviors apply to all nodes, with slight (uncontrollable) variations existing. The profile and bounded variations were written in the MATLAB code. One of the randomly simulated signals that happened to have close parameters to the tested signal was overlayed in Fig. 4 as an example of how close the model can be to the empirical data.

The bias current for each node is directly calculated from its respective channel resistance vector. The steep rise in current when the node is touched was generated with a line of slope (numerator) proportional to the maximum current. The saturation area where it levels off was approximated with $y = \sqrt{x}$. The linear rise due to thermal transfer while the node is touched was made to have a slope (denominator) be proportional to the maximum current. Finally, the signal immediately drops back to the bias current. All of these components that form the signal were given randomness within

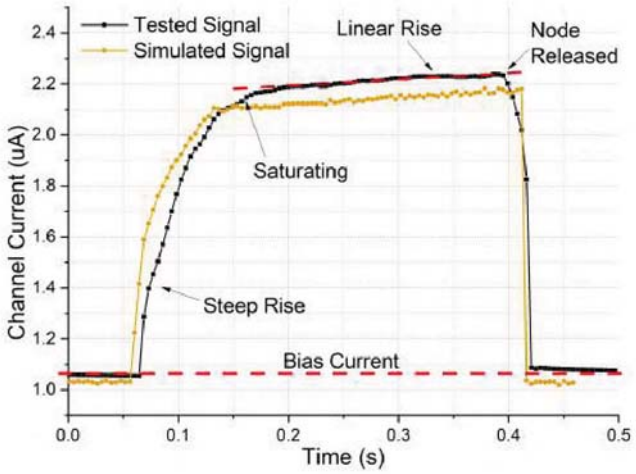

Fig. 4: The node response is empirically shown along with a simulated response from the MATLAB program with close parameters for comparison.

bounds expected from the actual signals. The timing of when the node is first touched, the rise time, saturation time, and duration of node touch were also randomly generated within set bounds.

IV. Simulation, Results and Analysis

After the nodes were modeled with random but bounded variations expected from real prints, the final signal I_S could be generated. A binary pattern mask was randomly created for each sample where 1 means that a node was touched and 0 means it was not touched. This serves as the target pattern (i.e. the training dataset) for each sample. Also, the binary pattern was multiplied with the nodes to suppress signals from being generated when a node is not touched. The resulting matrix contains all 16 node responses expressing randomized target pattern. The values of each node were then summed row-by-row to generate the signal, I_S. The full dataset is visualized in Fig. 5. The matrix has dimensions of $size(I_s) \times (18) \times (sample\,count)$.

The signal variability of the individual nodes and current I_S can be visualized in Fig. 6. The random variations of

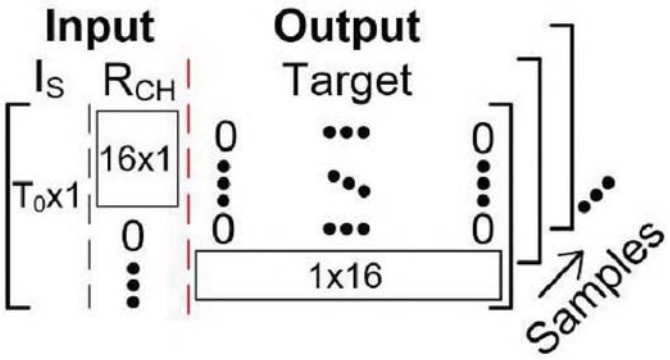

Fig. 5: The final dataset for testing and training the ESN is a matrix with dimensions of $size(I_s) \times (2+16) \times (sample\,count)$.

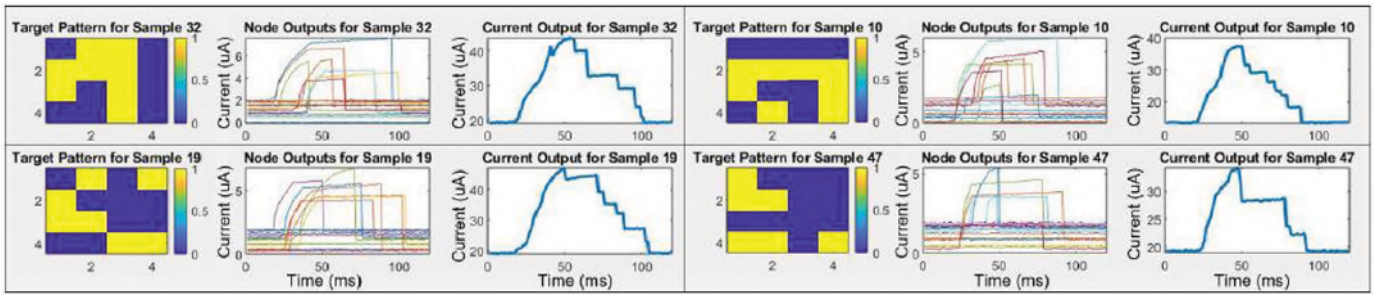

Fig. 6: The MATLAB simulation output shows the target pattern, nodal response, and final signal I_S (respectively) of four randomly selected samples.

the node signals can be adjusted to within specified ranges as more empirical data is collected. The inclusion of the channel resistances as an input feature will give the ESN the ability to classify which nodes were pressed. If the node resistances were identical, the ESN would only be able to distinguish how many nodes were pressed rather than resolving the actual pattern. The amount of samples needed for training will increase as the number of nodes increases. This means that training the ESN for a 2×2 or 3×3 grid array (as opposed to the 4×4 array of this paper) will require less samples and therefore less training time. If the ESN has too high of an error rate, the random variations may be reduced to simplify the uniqueness of input current signals. Forming a single model from the generated datasets of this sensor will provide a generalized pseudo-calibration technique for its stabilized performance.

V. Conclusion

Inkjet printed sensors and circuits made from minimally produced fabrication setups have certain inconsistencies that prevent highly reliable operation. A method of overcoming the inevitable variabilities is by using machine learning as a method of data stabilization. The echo state network of future works requires generation of input data to train and test the model. This report shows an minimally produced IJP tactile sensor printed with only silver nanoparticle ink using an office-quality inkjet printer. The node responses were modeled in MATLAB and then summed to generate the input signal (I_S) to the ESN. The channel resistances of the array are stored as an input feature such that the reservoir can resolve the touched pattern. Random binary target patterns were masked with the nodes and set as the output (training) signal to the ESN. The final dataset will be used to develop the ESN such that the IJP tactile sensor, and ultimately other IJP sensors, may have improved data stability.

VI. Acknowledgment

The work was supported in part by National Science Foundation (NSF) Award ECCS-1813949 and Award CNS-1645863.

References

[1] M. Gaskill, "Solving the challenges of long duration space flight with 3d printing," 2019. [Online]. Available: https://www.nasa.gov/mission_pages/station/research/news/3d-printing-in-space-long-duration-spaceflight-applications

[2] S. Singh, "Printed electronics market worth $19.8 billion by 2024," *Markets and Markets Research*, 2019. [Online]. Available: https://www.marketsandmarkets.com/PressReleases/printed-electronics-market.asp

[3] E. R. Garcia, "Inkjet printed microelectronic devices and circuits (doctoral dissertation)," *Universitat Autonoma de Barcelona*, 2014.

[4] V. Beedasy and P. J. Smith, "Printed electronics as prepared by inkjet printing," *Materials*, vol. 13, no. 3, 2020.

[5] S. Stoyanov and C. Bailey, "Machine learning for additive manufacturing of electronics," in *2017 40th International Spring Seminar on Electronics Technology (ISSE)*, Conference Proceedings, pp. 1–6.

[6] H. Jaeger, "A tutorial on training recurrent neural networks, covering bppt, rtrl, ekf and the "echo state network" approach," *Fraunhofer Institute for Autonomous Intelligent Systems (AIS)*, vol. GMD Report 159, 2002.

[7] W. Maass, T. Natschlager, and H. Markram, "Real-time computing without stable states: A new framework for neural based on perturbations," *Neural Computation*, vol. 14, p. 2531–2560, 2002.

[8] S. Muhlbacher-Karrer, A. H. Mosa, L. Faller, M. Ali, R. Hamid, H. Zangl, and K. Kyamakya, "A driver state detection system—combining a capacitive hand detection sensor with physiological sensors," *IEEE Transactions on Instrumentation and Measurement*, vol. 66, no. 4, pp. 624–636, 2017.

[9] M. J. Rahman and B. I. Morshed, "Improving accuracy of inkjet printed core body wrap temperature sensor using random forest regression implemented with an android app," in *2019 United States National Committee of URSI National Radio Science Meeting, USNC-URSI NRSM 2019, January 9, 2019 - January 12, 2019*, ser. 2019 United States National Committee of URSI National Radio Science Meeting, USNC-URSI NRSM 2019. Institute of Electrical and Electronics Engineers Inc., Conference Proceedings.

[10] F. Rasheed, M. Hefenbrock, M. Beigl, M. B. Tahoori, and J. Aghassi-Hagmann, "Variability modeling for printed inorganic electrolyte-gated transistors and circuits," *IEEE Transactions on Electron Devices*, vol. 66, no. 1, pp. 146–152, 2019.

[11] B. Ando, S. Baglio, C. O. Lombardo, and V. Marletta, "An inkjet printed sensor for load measurement," in *2014 IEEE Sensors Applications Symposium (SAS)*, Conference Proceedings, pp. 185–188.

[12] T. Yun, S. Eom, and S. Lim, "Paper-based capacitive touchpad using home inkjet printer," *Journal of Display Technology*, vol. 12, no. 11, pp. 1411–1416, 2016.

[13] T. Li and S. Zhang, "Inkjet-printed proximity sensor for humanrobot interaction," *Microsystem Technologies*, vol. 24, no. 12, pp. 4875–4880, 2018.

[14] S. Gardner, M. R. Haider, M. T. Islam, J. I. D. Alexander, and Y. Massoud, "Aluminum-doped zinc oxide (zno) inkjet-printed piezoelectric array for pressure gradient mapping," *62nd IEEE International Midwest Symposium on Circuits and Systems (MWSCAS 2019)*, 2019.

[15] S. D. Gardner, J. I. D. Alexander, Y. Massoud, and M. R. Haider, "An inkjet-printed paper-pased flexible sensor for pressure mapping applications," *IEEE International Symposium on Circuits and Systems (ISCAS 2020)*, 2020.

[16] H. Matsui, Y. Takeda, and S. Tokito, "Flexible and printed organic transistors: From materials to integrated circuits," *Organic Electronics*, vol. 75, 2019.

[17] J. R. Greer and R. A. Street, "Thermal cure effects on electrical performance of nanoparticle silver inks," *Acta Materialia*, vol. 55, no. 18, pp. 6345–6349, 2007.